Original Article

Identification of an energy metabolism-related six-gene signature for distinguishing and forecasting the prognosis of low-grade gliomas

Guoli Liu[1,2], Yuan Lu[3,4], Duangui Gao[4], Zhi Huang[3,4], Lin Ma[1,2]

[1]Medical School of Chinese People's Liberation Army, Beijing, China; [2]Department of Radiology, The First Medical Center of Chinese People's Liberation Army General Hospital, Beijing, China; [3]School of Basic Medical Science, Guizhou Medical University, Guiyang, China; [4]Department of Interventional Radiology, the Affiliated Hospital of Guizhou Medical University, Guiyang, China

Contributions: (I) Conception and design: G Liu, L Ma; (II) Administrative support: Z Huang, L Ma; (III) Provision of study materials or patients: Z Huang, L Ma; (IV) Collection and assembly of data: A Zhao, D Gao; (V) Data analysis and interpretation: G Liu, A Zhao; (VI) Manuscript writing: All authors; (VII) Final approval of manuscript: All authors.

Correspondence to: Dr. Zhi Huang. Department of Interventional Radiology, the Affiliated Hospital of Guizhou Medical University, Guiyang, China. Email: doctor@huangzhi.com; Dr. Lin Ma. Medical School of Chinese People's Liberation Army, Beijing, China. Email: cjr.malin@vip.163.com.

Background: Low-grade gliomas (LGG) account for 20–25% of all gliomas. In this study, we assessed whether metabolic status was correlated with clinical outcomes in LGG patients using data from The Cancer Genome Atlas (TCGA).

Methods: LGG patient data were collected from TCGA, and the Molecular Signature Database was used to extract gene sets related to energy metabolism. After performing a consensus-clustering algorithm, the LGG patients were divided into four clusters. We then compared the tumor prognosis, function, immune cell infiltration, checkpoint proteins, chemo-resistance, and cancer stem cells (CSC) between the two groups with the greatest prognostic difference. Using least absolute shrinkage and selection operator (LASSO) analysis, an energy metabolism-related signature was further developed.

Results: Energy metabolism-related signatures were applied to identify four clusters (C1, C2, C3, and C4) using a consensus-clustering algorithm. C1 LGG patients were more related to the synapse and had higher CSC scores, more chemo-resistance, and a better prognosis. C4 LGG was observed to have more immune-related pathways and better immunity. We then identified six energy metabolism-related genes (*PYGL*, *HS3ST3B*, *NNMT*, *FMOD*, *CHST6*, and *B3GNT7*) that can accurately predict LGG prognosis not only as a whole but also based on the independent predictions of each of these six genes.

Conclusions: The energy metabolism-related subtypes of LGG were identified, which were strongly related to the immune microenvironment, immune checkpoint proteins, CSCs, chemo-resistance, prognosis, and LGG advancement. A signature of genes involved in energy metabolism could help to distinguish and predict the prognosis of LGG patients, and a promising method to discover patients that may benefit from LGG therapy.

Keywords: Low-grade gliomas (LGGs); prognosis; metabolic status; signature

Submitted Nov 29, 2022. Accepted for publication Jan 29, 2023. Published online Feb 15, 2023.
doi: 10.21037/atm-22-6502
View this article at: https://dx.doi.org/10.21037/atm-22-6502

Introduction

Low-grade gliomas (LGGs) are slow-growth primary brain tumors that account for 20–25% of all gliomas, with an average survival of 5–15 years (1). According to the classification of the World Health Organization (WHO), low-grade glioma mainly refers to grade I and II neuroepithelial tumors. It includes hairy cell astrocytoma, neurocytoma, astrocytoma and mixed oligodendrocytoma (2). As with the deepening of research on LGG, many aspects related to clinical diagnosis and treatment remain controversial (3,4). For a long time, LGGs have been considered a subgroup of gliomas with benign clinical and biological behaviors, but growing evidence shows that the same grade gliomas have biological behaviors and clinical characteristics (5,6). However, the prognosis is quite different; some patients can survive for a long time or have a long survival period, while others have a highly malignant outcome, even similar to that of glioblastoma multiforme (7). Therefore, accurate risk assessment and selective diagnostic/treatment strategies are necessary.

The different energy metabolism of cancer cells compared to normal cells is a hallmark of most cancers (8,9). Growing evidence suggests that energy metabolism reprogramming is tightly related to cancer initiation and advancement, especially aerobic glycolysis (10,11). Aerobic glycolysis may provide enough adenosine triphosphate (ATP) for tumors under hypoxia, playing a crucial role in tumor growth, metastasis, and therapy (10,12,13).

Highlight box

Key findings

- The energy metabolism-related subtypes of LGG were identified, which were closely associated with the immune microenvironment, the expression of immune checkpoints, cancer stem cells (CSCs), chemotherapy resistance, prognosis, and LGG progression.

What is known and what is new?

- The same grade gliomas have biological behaviors and clinical characteristics.
- We assessed whether metabolic status was correlated with clinical outcomes in LGG patients using data from The Cancer Genome Atlas (TCGA).

What is the implication, and what should change now?

- LGG prognosis can be accurately predicted using the six energy metabolism-related genes (*PYGL*, *HS3ST3B*, *NNMT*, *FMOD*, *CHST6*, and *B3GNT7*) altogether as well as based on the independent predictions of each of these six genes.

Some tumor cells exhibit a predominant glycolysis phenotype, while others display a predominant oxidative phosphorylation (OXPHOS) phenotype (14). Metabolic reprogramming in cancer cells is increasingly being shown to be heterogeneous (15). In addition to absorbing free fatty acids and ketones, tumor cells can also absorb catabolic acids produced by their neighbors as energy sources for mitochondrial oxidative phosphorylation (16,17). Furthermore, glutamate-driven mitochondrial oxidative phosphorylation, as opposed to glycolysis, accounts for most ATP production under hypoxic conditions (18). Recent research suggests that cancer-related alterations in energy metabolism may lead to new targeted therapies, which may be less harmful and more effective in treating cancer compared to conventional cytotoxic chemotherapy (19,20).

Similarly, LGG cells also provide energy for life activities mainly by glycolysis instead of aerobic respiration. It was found that the expression and activity of key glycolytic enzymes in LGG cells increased, and glucose absorption and lactic acid production increased significantly. The significant increase of glycolysis metabolism increases the growth rate, invasion and metastasis ability of LGG cells, and promotes the progress of LGG disease (21). Research shows that the factors causing tumor occurrence, such as the deletion of tumor suppressor gene and the activation of proto oncogene, can cause metabolic changes of tumor cells, and lead to aerobic glycolysis disorder, which can lead to tumor progression (22). As low-grade gliomas are mainly characterized by their IDH mutations, IDH1 and IDH2 are NADP+-dependent enzymes that catalyze the oxidative decarboxylation of isocitrate in the citric acid cycle to α-Ketoglutarate (α-KG). In glioma, IDH mutation causes the enzyme to α- KG is further converted to 2-hydroxyglutarate (2-HG). 2-HG and α-KG antagonizes, competitively inhibits multiple α-KG dependent dioxygenase activity, resulting in chromatin hypermethylation (23,24). Berghoff *et al.* (25) also found a strong association between IDH1 mutation status and the tumor immune microenvironment in LGG. Patients with mutated IDH1 had higher immune cell infiltration and higher expression levels of programmed cell death ligand 1 (PD-L1) than patients with non mutated IDH1 IDH1 mutation can be used as a risk indicator for the prognosis of LGG.

The present study summarizes the molecular typing of LGGs based on metabolic gene signatures and the construction of risk prediction models, providing new perspectives for the early detection, prognosis, and optimization of treatment options for LGGs. We present

the following article in accordance with the TRIPOD reporting checklist (available at https://atm.amegroups.com/article/view/10.21037/atm-22-6502/rc).

Methods

Acquisition of information on patients with LGG

Data from 510 LGG patients, including transcriptomic datasets and relevant clinical information, were collected from The Cancer Genome Atlas (TCGA, www.portal.gdc.com). The study was conducted in accordance with the Declaration of Helsinki (as revised in 2013).

Selection of energy metabolism-related genes and consensus clustering

Data on energy metabolism genes were collected from the Molecular Signatures Database (MSigDB) (www.broad.mit.edu/gsea/msigdb/) (14,26). After removing the overlapping genes, 590 genes related to energy metabolism were retrieved. Consensus clustering was performed using "ConsensusClusterPlus" (v1.54.0) (cluster size: 6). Heatmaps were created using "pheatmap" (v1.0.12) to visualize gene expression. Survival was assessed using Kaplan-Meier curves generated by the "survival" R package.

Differentially expressed genes (DEGs) recognition and enrichment assay

To understand the DEGs between the groups, volcano plots (fold change >4.0 or <0.25, P<0.05) were drawn to illustrate the abundance of DEGs using "ggplot". The top 50 up- or down-regulated DEGs were displayed as a heatmap. For a deeper understanding of the functions of involved genes, enrichment analysis was carried out using "ClusterProfiler". Gene Ontology (GO) and the Kyoto Encyclopedia of Genes and Genomes (KEGG) were also analyzed with "ClusterProfiler". Furthermore, the one-class logistic regression (OCLR) algorithm was applied to highlight the relationship between metabolic status and CSCs, as previously described (27).

Investigation of immune infiltration and immune checkpoints

The groups were consensus-clustered, and immune infiltration was estimated using CIBERSORT in 'immunedeconv' and displayed as heatmaps and boxplots. In addition, eight immune checkpoint-related genes were selected, including *CD274*, *PDCD1*, *PDCD1LG2*, *CTLA4*, *LAG3*, *HAVCR2*, *TIGIT*, and *SIGLEC15*, and the gene levels were extracted and visualized using the "ggplot2" and "pheatmap" R packages. Data were analyzed using the Wilcox test, and P<0.05 was considered statistically significant.

Gene signature identification

The DEGs between groups were obtained as three gene sets. Energy metabolism-related genes were selected using a Venn diagram with these three gene sets and 590 energy metabolism-related genes. Using univariate Cox regression, LGG data were screened to determine whether genes associated with energy metabolism could predict overall survival in patients. Additionally, LASSO Cox regression was applied to select features through glmnet. A Kaplan-Meier assay was performed using log-rank tests and univariate cox regression.

Results

Data collection and consensus clustering

To explore the involvement of energy metabolism in LGG, the clinical information and RNA test data of 510 patients were collected from TCGA. Subsequently, 590 energy metabolism-related genes (EMRGs) were identified. To further investigate how EMRGs affect LGG prognosis, an empirical cumulative distribution function (CDF) plot, principal components analysis (PCA), and a consensus clustering matrix showed that LGG patients were divided into four groups (*Figure 1A-1D* and available online: https://cdn.amegroups.cn/static/public/atm-22-6502-1.xlsx). DEGs [standard deviation (SD) >0.1] grouped by EMRGs were shown in these two groups (*Figure 1E* and available online: https://cdn.amegroups.cn/static/public/atm-22-6502-1.xlsx). Among the LGG patients in clusters 1 to 4, the median overall survival was 10.3, 7.3, 4.7, and 1.7 years (P<0.0001, *Figure 1F* and available online: https://cdn.amegroups.cn/static/public/atm-22-6502-1.xlsx), and progression-free survival was 6.3, 3.6, 4.1, and 1.1 years (P<0.0001, Figure S1), respectively.

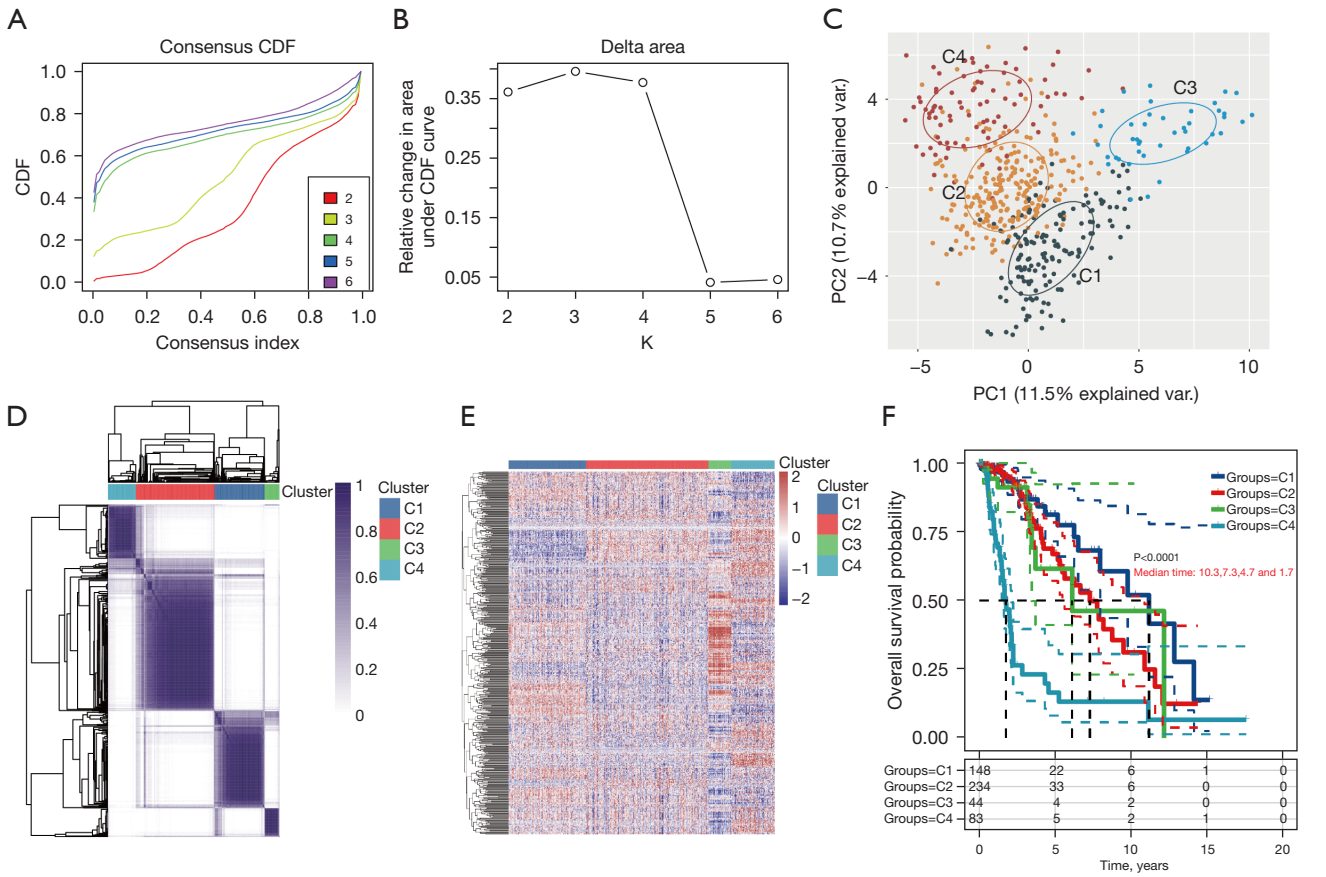

Figure 1 Subtypes of LGG patients based on the EMRG consensus cluster. (A) CDF plot for k=2 to 6. (B) AUC changes. (C) Principal component analysis of the different clusters. (D) Consensus clustering matrix of 510 LGG patients for k=4. The darker the blue stand for the higher the expression of gene set. (E) Heatmap of gene expression related to energy metabolism. Red/blue: high/low gene expression. (F) Kaplan-Meier survival curves of overall survival in the different clusters. LGG, low-grade gliomas; EMRG, energy metabolism-related gene; CDF, cumulative distribution function; AUC, area under the curve.

Enrichment analysis

To investigate the different mechanisms between the clusters, we identified the DEGs in clusters 1 and 4 with the largest differences in overall survival. The volcano plot displayed the up-regulated genes (*CACNG2*, *TRIM67*, *SCRT1*, *PRLHR*, etc.) and down-regulated genes (*PDPN*, *EMP3*, *CH3L1*, *TIMP1*, etc.) in cluster 1 compared to cluster 4 (*Figure 2* and available online: https://cdn.amegroups.cn/static/public/atm-22-6502-2.xlsx). Next, the top 50 genes were displayed as a heatmap in order of their up- and down-regulation (*Figure 2B* and available online: https://cdn.amegroups.cn/static/public/atm-22-6502-2.xlsx). In addition, the threshold and adjusted P value of the reduced change value were set at 4 and 0.05, respectively, and functional enrichment analysis was conducted based on the up- and down-regulated genes.

As shown in *Figure 2C*,*2E*, the major signaling pathway in cluster 1 shown by KEGG analysis was mainly related to activating the synaptic transmission processes and down-regulating the immune-related functions. The biological process of GO analysis showed a similar result, with the major enriched terms closely associated with the activated synaptic transmission in up-regulated genes (*Figure 2D* and available online: https://cdn.amegroups.cn/static/public/atm-22-6502-2.xlsx) and immune cell proliferation in down-regulated genes (*Figure 2F* and available online: https://cdn.amegroups.cn/static/public/atm-22-6502-2.xlsx).

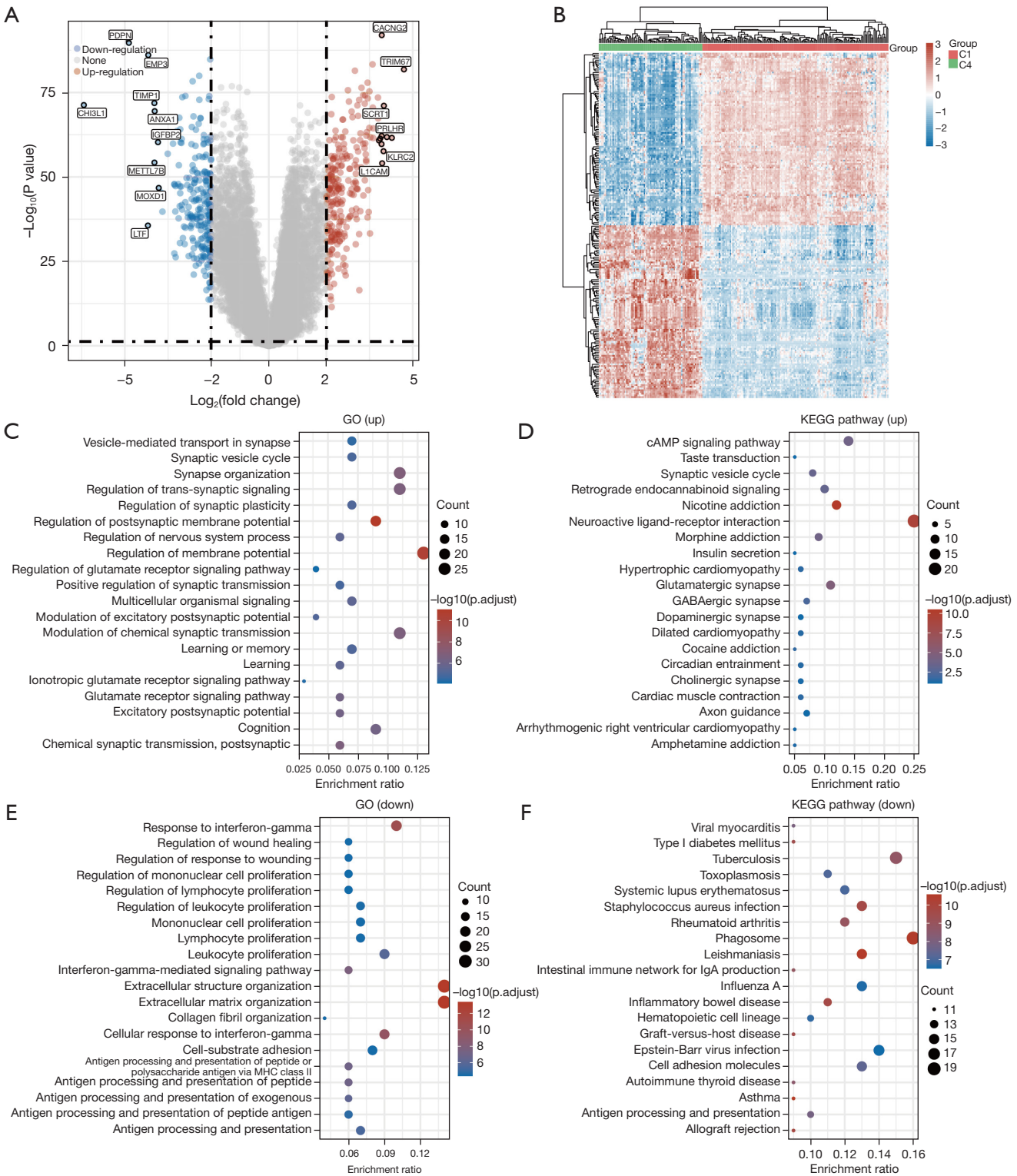

Figure 2 Identification of DEGs and enrichment analysis between clusters 1 and 4. (A) Volcano plot of DEGs. Red/blue: up-/down-regulated genes. (B) Top 50 DEGs. Red/blue: high/low gene expression. In cluster 1, (C) GO analysis of the up-regulated genes, (D) KEGG pathway analysis of the up-regulated genes, (E) GO analysis of the down-regulated genes, (F) KEGG pathway analysis of the down-regulated genes. DEGs, differentially expressed genes; GO, Gene Ontology; KEGG, Kyoto Encyclopedia of Genes and Genomes.

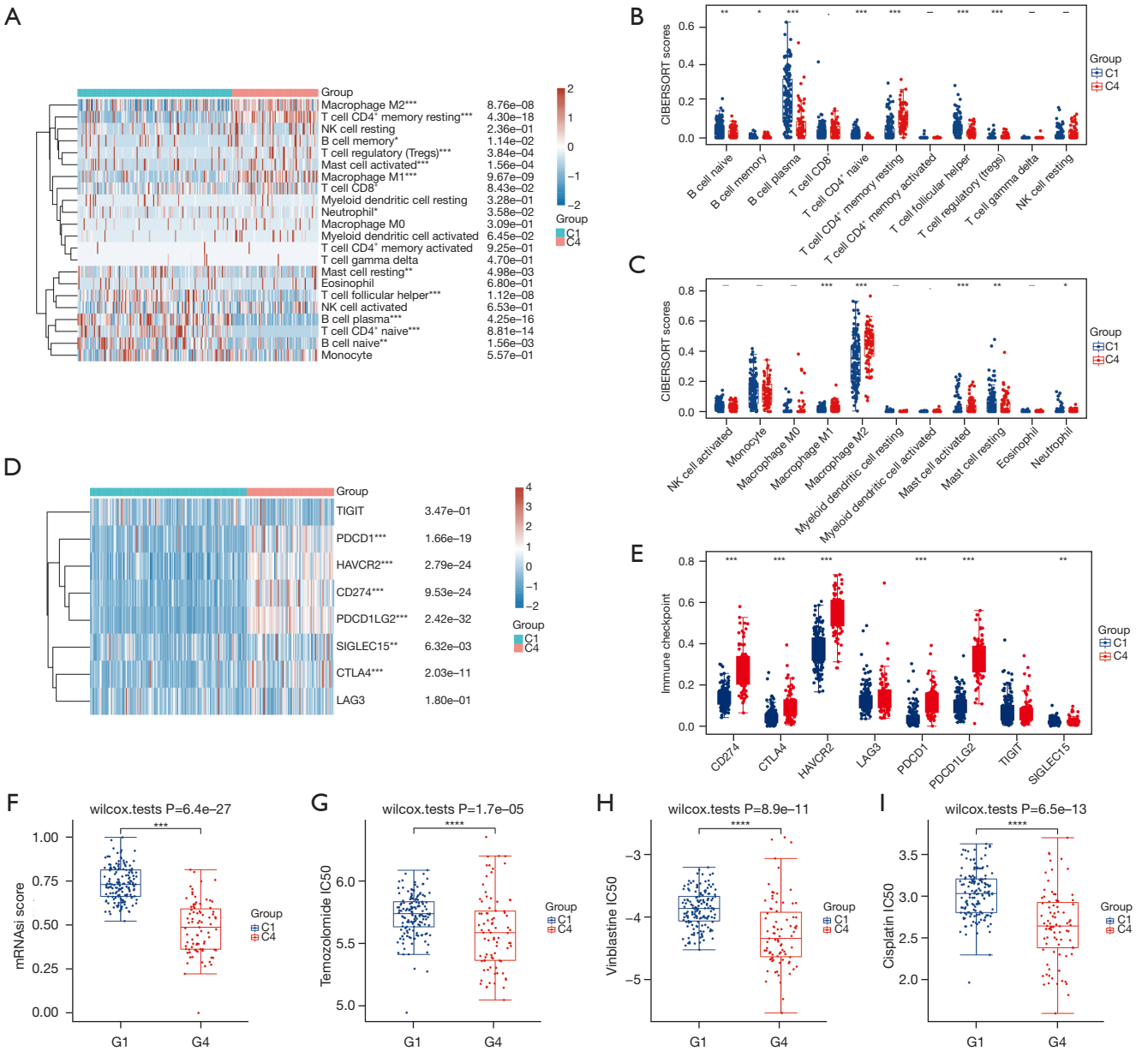

Figure 3 Analysis of the immune cell infiltration in clusters 1 and 4. (A) Heatmap of immune cell scoring using the CIBERSORT algorithm. Red/blue represents high/low expression or score. (B) Boxplots of immune infiltration status using the CIBERSORT algorithm. Boxplot (C) and Heatmap (D) of IC-related gene expression. The "-" represents no statistical significance. Red/blue represents high/low expression or score. (E) Boxplot of immune checkpoint-related genes expression in two clusters. CSC score (F) and chemoresistance of the two clusters to temozolomide (G), vinblastine (H), and cisplatin (I). *P<0.05, **P<0.01, ***P<0.001, ****P<0.0001. CSC, cancer stem cells; IC, immune checkpoint.

Immune infiltration assay

The up-regulated genes in cluster 4 were closely related to tumor immunity. The immuno-infiltration heatmap revealed markedly different tumor immune microenvironments (*Figure 3A*, available online: https://cdn.amegroups.cn/static/public/atm-22-6502-3.xlsx). The boxplots using the CIBERSORT algorithm also showed similar results (*Figure 3B,3C*, available online: https://cdn.

amegroups.cn/static/public/atm-22-6502-3.xlsx). Moreover, the expressions of immune checkpoint (IC)-related genes were higher in cluster 4 (*Figure 3D*,*3E*, available online: https://cdn.amegroups.cn/static/public/atm-22-6502-3.xlsx). These results indicated a close link between EMRGs and immune checkpoint biomarkers, which may contribute to LGG immunotherapy.

CSCs and drug sensitivity analysis

Analysis of the CSCs of 11,774 CSC-related gene profiles indicated that the CSC scores were higher in cluster 1 patients, suggesting a link between energy metabolism and CSC scores (*Figure 3F* and available online: https://cdn.amegroups.cn/static/public/atm-22-6502-3.xlsx). Next, drug susceptibility was assessed in the two clusters. Furthermore, the energy metabolism status was closely related to the half maximal inhibitory concentration (IC50) scores of temozolomide, vinblastine, and cisplatinin LGG patients (*Figure 3G-3I* and available online: https://cdn.amegroups.cn/static/public/atm-22-6502-3.xlsx).

Identification of the genetic prognostic markers associated with energy metabolism

Considering that LGG prognosis is closely related to energy metabolism status, an EMRG-based prognostic signature (EMRGPS) was constructed for prognostic evaluation. A Venn diagram was constructed using the DEGs between the four clusters, and 11 EMRGs were identified from the total EMRGs and four clusters (*Figure 4A* and available online: https://cdn.amegroups.cn/static/public/atm-22-6502-4.xlsx). More importantly, these 11 EMRGs s were significantly associated with the overall survival of LGG.

To verify the feasibility and stability of clinical prognostications using these 11 genes, we performed LASSO analysis and obtained six EMRGs (*PYGL*, *HS3ST3B*, *NNMT*, *FMOD*, *CHST6*, and *B3GNT7*) that were associated with the prognosis of LGG patients (*Figure 4B*,*4C*, available online: https://cdn.amegroups.cn/static/public/atm-22-6502-4.xlsx). We then calculated the EMRGPS risk scores of the energy metabolism-related genes based on the Cox coefficients. A group of LGG patients could be categorized into low- or high-risk groups based on risk scores (*Figure 4D*, available online: https://cdn.amegroups.cn/static/public/atm-22-6502-4.xlsx). As shown in the Kaplan-Meier curve, high-risk patients exhibited drastically poorer overall survival (*Figure 4E*, available online: https://cdn.amegroups.cn/static/public/atm-22-6502-4.xlsx), with areas under the curves (AUCs) for 1-, 3-, and 5-year overall survival of 0.874, 0.835, and 0.728, respectively (*Figure 4F*, available online: https://cdn.amegroups.cn/static/public/atm-22-6502-4.xlsx).

In addition, LGG tissues showed a higher expression of the six EMRGs compared to healthy tissues (*Figure 5* and available online: https://cdn.amegroups.cn/static/public/atm-22-6502-5.xlsx).

Identification of the independent genetic prognostic markers associated with energy metabolism

To further confirm the role of the above six EMRGs in prognostic assessment, LASSO analysis was performed, and each of those six genes was found to be associated with LGG prognosis. LGG patients could be separated into low- or high-risk groups according to the risk scores. For each of these six genes, the Kaplan-Meier assay indicated that high-risk patients had worse overall survival (*Figure 6A-6F*, available online: https://cdn.amegroups.cn/static/public/atm-22-6502-6.xlsx). Also, the AUCs of these six genes for 1-year overall survival were 0.834, 0.852, 0.836, 0.807, 0.786, and 0.794, respectively. For *PYGL*, *HS3ST3B*, *NNMT*, *FMOD*, *CHST6*, and *B3GNT7*, the predicted AUC 1-year overall survival was 0.834, 0.852, 0.836, 0.807, 0.786, and 0.794, respectively; the 3-year overall survival was 0.79, 0.773, 0.77, 0.746, 0.718, and 0.743, respectively; and the 5-year overall survival was 0.724, 0.773, 0.662, 0.675, 0.584, 0.675, and 0.682, respectively (*Figure 6G-6L*, available online: https://cdn.amegroups.cn/static/public/atm-22-6502-6.xlsx). These results indicated that these six genes had a stable and independent predictive capacity.

Discussion

Cancer cells acquire large amounts of ATP through efficient glycolysis rather than oxidative phosphorylation, even in the presence of oxygen, creating a favorable microenvironment and proliferative advantage for tumor cells, a phenomenon first described as the Warburg effect (28). Since then, cancer researchers have exerted significant efforts to understand the mechanisms underlying metabolic reprogramming (10,29). Increasing evidence suggests that the metabolism of cancer patients is affected by drugs targeting multiple cellular energetics pathways (30). Herein, based on TCGA database, an evaluation of how energy metabolism affects LGG prognosis was conducted. Clinicopathological features

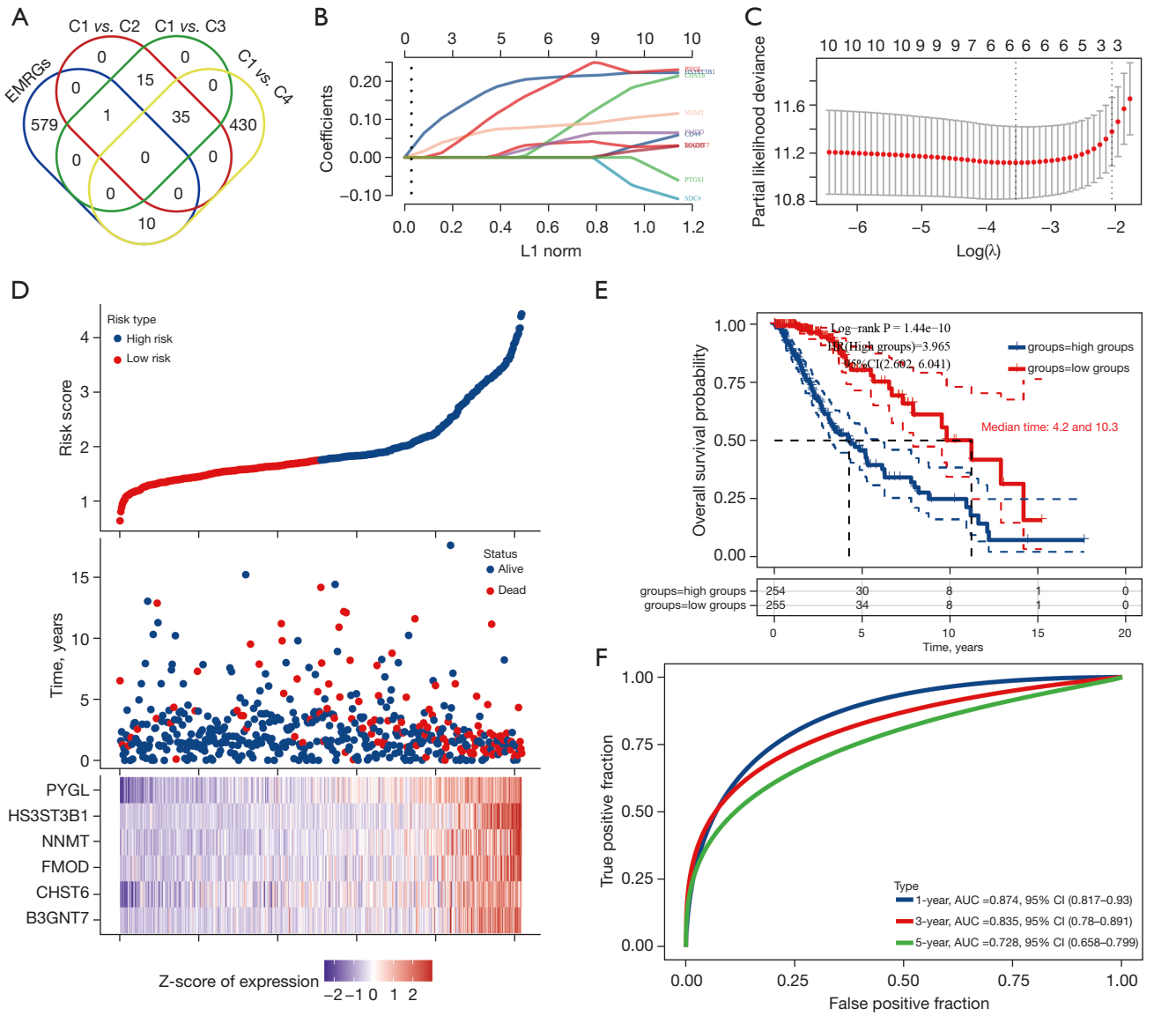

Figure 4 Prognostic predictive signatures of six EMRGs. (A) Screening of eleven candidate EMRGs. (B) LASSO coefficient profiles of eleven EMRGs. (C) Partial likelihood deviance was plotted *vs.* log lambda. (D) Risk score for each sample based on EMRGs. LGG patients were separated into low-/high-risk according to the risk scores. The levels of six genes associated with the prognostic features in each sample are displayed in red and blue, respectively. (E) Kaplan-Meier survival curves. (F) AUC of the risk score signature in the ROC analysis. EMRG, energy metabolism-related gene; LASSO, least absolute shrinkage and selection operator; LGG, low-grade gliomas; ROC, receiver operating characteristic; AUC, area under the curve; CI, confidence interval.

are closely associated with energy metabolism, suggesting that it is significantly related to LGG.

Tumor cells adopt aerobic glycolysis to meet their own demand of rapid proliferation, closely related to the microenvironment of tumors. Because in the process of rapid tumor proliferation, the number of original blood vessels can't meet the needs of the tumor itself to grow, the oxygen supply is severely insufficient. Whereas under hypoxia, glycolysis rapidly generates energy needed for cell proliferation. Interestingly, the hypoxic microenvironment present at the periphery of tumor cells activates the hypoxia inducible factor (HIF) family of proteins and upregulates

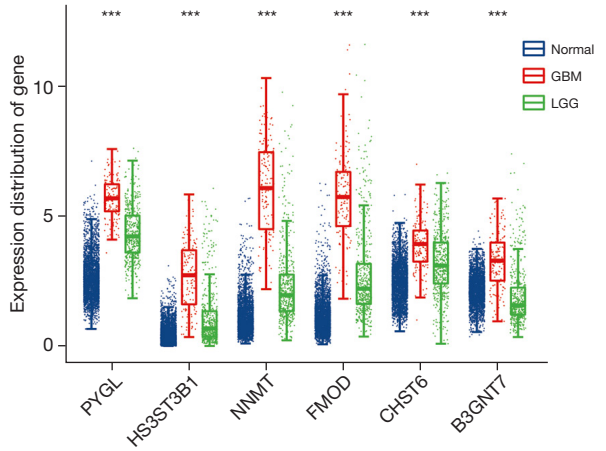

Figure 5 Expression patterns of the six metabolism-related genes associated with LGG prognosis. Expression patterns of the six genes in normal, GBM, and LGG tissue. ***P<0.001. GBM, glioblastoma; LGG, low-grade gliomas.

glucose transporters and multiple enzymatic activities of the glycolytic pathway, thereby exacerbating the utilization of glycolysis until sufficient oxygen is provided after angiogenesis. Whereas afterwards the cells enter a period of accelerated division again resulting in hypoxia, such a vicious cycle causes the longer the tumor cell grows, and even generates invasive capacity (31). Thus enabling tumour cells to gain a proliferative advantage, escape immune surveillance or reduce the apoptosis of mutations, may all be selectively retained during rapid cell proliferation (32). Such as the P53 gene is one of the important tumor suppressors and an important gene related to metabolism. TP53 mutations can lead to chromosomal/genomic mutational instability and thereby elevate tumor mutational burden (TMB). Examination of immune factors revealed that TMB levels were correlated with natural killer cell levels, anti-inflammatory factor ratios, and M1/M2 macrophage ratio levels. So TP53 mutated tumor cells are more prone to immune escape, which leads to tumor cell infiltration (33).

According to the functional enrichment analysis, energy metabolism and inflammatory responses were intimately related, indicating a relationship between energy metabolism and the tumor immune microenvironment. Recently, various groups have reported several changes in the metabolic status of LGG, suggesting that metabolic status might contribute to the tumor immune microenvironment (34,35). Some reports have demonstrated that immunity is influenced by lactate accumulation during aerobic glycolysis in tumor cells, including enhanced cytokine transcription and the inhibition of monocyte-to-dendritic cell differentiation (36,37). Moreover, mitochondrial metabolic reprogramming can trigger immunogenic cell death (ICD) and increase the effectiveness of chemotherapy in cancer by increasing OXPHOS (38). Similar results were shown in our study: metabolic status was closely linked to chemo-resistance to chemotherapeutic agents, including temozolomide, vinblastine, or cisplatin. Our findings also highlighted that many of the immune checkpoint inhibitor biomarkers exhibited a significant relationship with energy metabolism, which are useful as biomarkers and even contribute to the progression of LGG. Checkpoint inhibitors for LGG have provided considerable achievements, which could change the paradigm of LGG treatment (39). As a result of this study, it is suggested that the energy metabolism status might influence the tumor microenvironment by influencing immune cell infiltration, which might play a key role in LGG carcinogenesis by influencing immunotherapy sensitivity and resistance.

Using the OCLR algorithm (40), we revealed that the metabolic status of LGG is closely related to CSCs, which are a class of undifferentiated cells with stem cell properties and high tumorigenicity, contributing to cancer heterogeneity and recurrence in LGG (41). Conventional treatments such as chemotherapy, radiotherapy, and immunotherapy have proven ineffective in combatting CSCs. However, the underlying mechanisms of CSC in the energy metabolism state of LGG patients require further investigation.

It is very important to search for the early diagnosis and prognostic indicators of LGG. In recent years, studies have suggested that ATRX mutation is related to the progression of brain glioma. ATRX mutation is common in grade II astrocytoma, and most of them have p53 gene mutation at the same time. Without p53 gene mutation, ATRX deletion will not cause brain tumors. The occurrence and progression of brain glioma is the result of IDH mutation and deletion of p53 and ATRX expression. In particular, ATRX deletion can lead to the mutation of relevant copy numbers and promote the progression of glioma (42). The expression of TPX2 is different between normal tissues and LGG tissues, and the expression of TPX2 in LGG tissues is significantly higher than that in normal tissues, and TPX2 expression is a risk factor for poor prognosis of LGG (43). Therefore, the expression level of ATRX, TPX2 and other genes is closely related to the prognosis of LGG. Owing to the strong link between energy

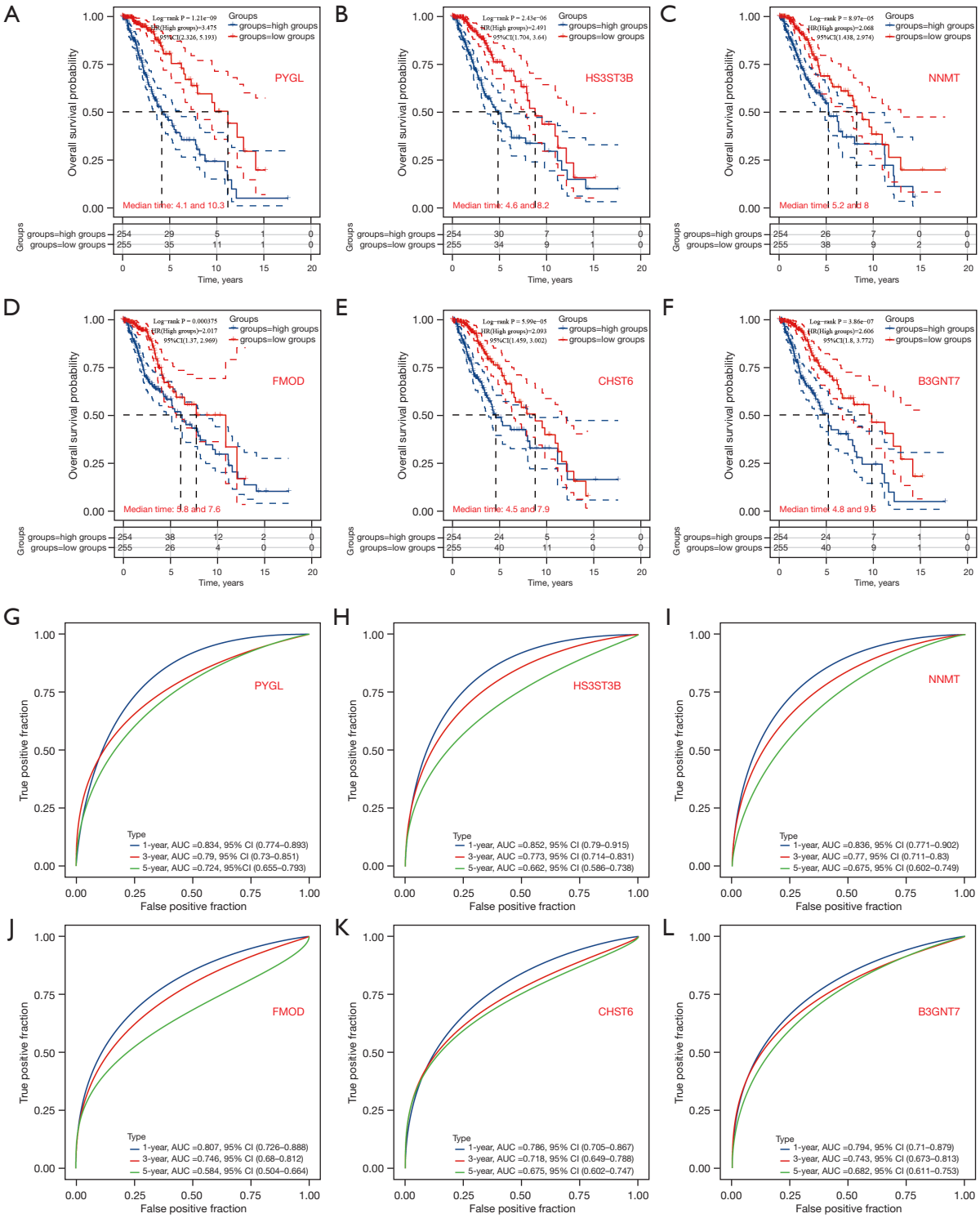

Figure 6 Independent prognostic prediction signatures of six energy metabolism-related genes. Kaplan-Meier survival curves of overall survival in *PYGL* (A), *HS3ST3B* (B), *NNMT* (C), *FMOD* (D), *CHST6* (E), and *B3GNT7* (F). AUC of the risk score signature in ROC analysis of *PYGL* (G), *HS3ST3B* (H), *NNMT* (I), *FMOD* (J), *CHST6* (K), and *B3GNT7* (L). CI, confidence interval; AUC, area under the curve.

metabolism and the clinicopathological features of LGG, a signature was constructed to classify patients with poor prognoses. Combining LASSO regression, we found that the signature of six genes (*PYGL*, *HS3ST3B1*, *NNMT*, *FMOD*, *CHST6*, and *B3GNT7*) had a substantial effect on survival. Among these genes, we found that *PYGL*, *NNMT*, and *CHST6* were differentially expressed between normal/tumor tissues. *PYGL* encodes glycogen phosphorylase, which are related to an increased risk of CRCs (44). *HS3ST3B1* encodes heparan sulfate 3-O-sulfotransferases, which are involved in neuronal axonogenesis (45). *NNMT*, which encodes Nicotinamide N-methyltransferase, drives metabolic remodeling and is associated with chemotherapy and radiotherapy resistance (46,47). FMOD encodes fibromodulin, which regulates glioma cell migration by activating the FAK-Src-Rho-ROCK signaling pathway in glioblastoma (48). *CHST6*, which encodes a carbohydrate sulfotransferase, leads to macular corneal dystrophy (49,50). Finally, *B3GNT7* encodes glycoconjugates, which can reduce the motility of lung cancer cell lines (51).

In summary, this study showed that the status of energy metabolism is strongly associated with the immune-microenvironment, IC-associated genes, CSCs, chemoresistance, prognosis, and recurrence of LGG. Gene signatures related to energy metabolism were constructed to predict the prognosis in LGG patients. For precision medicine, this feature can satisfy clinical needs for LGG management to a certain extent.

Conclusions

LGG prognosis can be accurately predicted using the six energy metabolism-related genes (*PYGL*, *HS3ST3B*, *NNMT*, *FMOD*, *CHST6*, and *B3GNT7*) altogether as well as based on the independent predictions of each of these six genes.

Acknowledgments

Funding: This study was supported by the Science and Technology Project of Baiyun District, Guiyang (No. [2019]36#); the Guizhou Province Science and Technology Planning Project Guizhou Genetic Basis-ZK[2021] General 489; and the Science and Technology Department of Guizhou Province [Guizhou specific Grant (2019) 4008].

Footnote

Reporting Checklist: The authors have completed the TRIPOD reporting checklist. Available at https://atm.amegroups.com/article/view/10.21037/atm-22-6502/rc

Conflicts of Interest: All authors have completed the ICMJE uniform disclosure form (available at https://atm.amegroups.com/article/view/10.21037/atm-22-6502/coif). The authors have no conflicts of interest to declare.

Ethical Statement: The authors are accountable for all aspects of the work, including ensuring that any questions related to the accuracy or integrity of any part of the work are appropriately investigated and resolved. The study was conducted in accordance with the Declaration of Helsinki (as revised in 2013).

References

1. Bosma I, Douw L, Bartolomei F, et al. Synchronized brain activity and neurocognitive function in patients with low-grade glioma: a magnetoencephalography study. Neuro Oncol 2008;10:734-44.
2. Wesseling P, Capper D. WHO 2016 Classification of gliomas. Neuropathol Appl Neurobiol 2018;44:139-50.
3. Dono A, Ballester LY, Primdahl D, et al. IDH-Mutant Low-grade Glioma: Advances in Molecular Diagnosis, Management, and Future Directions. Curr Oncol Rep 2021;23:20.
4. Harrabi SB, von Nettelbladt B, Gudden C, et al. Radiation induced contrast enhancement after proton beam therapy in patients with low grade glioma - How safe are protons? Radiother Oncol 2022;167:211-8.
5. Dimou J, Kelly J. The biological and clinical basis for early referral of low grade glioma patients to a surgical neuro-oncologist. J Clin Neurosci 2020;78:20-9.
6. Wang Z, Xiao X, Zhang Z, et al. A Radiomics nomogram for preoperative predicting recurrence of low grade gliomas based on multiparametric MRI. Research Square 2021. doi: 10.21203/rs.3.rs-345383/v1.

7. Ziu M, Kim BYS, Jiang W, et al. The role of radiation therapy in treatment of adults with newly diagnosed glioblastoma multiforme: a systematic review and evidence-based clinical practice guideline update. J Neurooncol 2020;150:215-67.
8. Hanahan D, Weinberg RA. Hallmarks of cancer: the next generation. Cell 2011;144:646-74.
9. Fumarola C, Petronini PG, Alfieri R. Impairing energy metabolism in solid tumors through agents targeting oncogenic signaling pathways. Biochem Pharmacol 2018;151:114-25.
10. Vander Heiden MG, DeBerardinis RJ. Understanding the Intersections between Metabolism and Cancer Biology. Cell 2017;168:657-69.
11. Liang L, Sun F, Wang H, et al. Metabolomics, metabolic flux analysis and cancer pharmacology. Pharmacol Ther 2021;224:107827.
12. Chang X, Liu X, Wang H, et al. Glycolysis in the progression of pancreatic cancer. Am J Cancer Res 2022;12:861-72.
13. Passaniti A, Kim MS, Polster BM, et al. Targeting mitochondrial metabolism for metastatic cancer therapy. Mol Carcinog 2022;61:827-38.
14. Zhou Z, Huang R, Chai R, et al. Identification of an energy metabolism-related signature associated with clinical prognosis in diffuse glioma. Aging (Albany NY) 2018;10:3185-209.
15. Hay N. Reprogramming glucose metabolism in cancer: can it be exploited for cancer therapy? Nat Rev Cancer 2016;16:635-49.
16. Bonuccelli G, Tsirigos A, Whitaker-Menezes D, et al. Ketones and lactate "fuel" tumor growth and metastasis: Evidence that epithelial cancer cells use oxidative mitochondrial metabolism. Cell Cycle 2010;9:3506-14.
17. Nieman KM, Kenny HA, Penicka CV, et al. Adipocytes promote ovarian cancer metastasis and provide energy for rapid tumor growth. Nat Med 2011;17:1498-503.
18. Fan J, Kamphorst JJ, Mathew R, et al. Glutamine-driven oxidative phosphorylation is a major ATP source in transformed mammalian cells in both normoxia and hypoxia. Mol Syst Biol 2013;9:712.
19. DeBerardinis RJ, Chandel NS. Fundamentals of cancer metabolism. Sci Adv 2016;2:e1600200.
20. Luengo A, Gui DY, Vander Heiden MG. Targeting Metabolism for Cancer Therapy. Cell Chem Biol 2017;24:1161-80.
21. Poff A, Koutnik AP, Egan KM, et al. Targeting the Warburg effect for cancer treatment: Ketogenic diets for management of glioma. Semin Cancer Biol 2019;56:135-48.
22. Qiao Q, Wang Y, Zhang R, et al. Autophagy related DNA methylation signature predict clinical prognosis and immune microenvironment in low-grade glioma. Transl Cancer Res 2022;11:2157-74.
23. Youssef G, Miller JJ. Lower Grade Gliomas. Curr Neurol Neurosci Rep 2020;20:21.
24. Wang WJ, Lu YJ, Li Y, et al. Construction of ceRNA networks with different types of IDH1 mutation status in low-grade glioma patients. Ann Transl Med 2022;10:254.
25. Berghoff AS, Kiesel B, Widhalm G, et al. Correlation of immune phenotype with IDH mutation in diffuse glioma. Neuro Oncol 2017;19:1460-8.
26. Subramanian A, Tamayo P, Mootha VK, et al. Gene set enrichment analysis: a knowledge-based approach for interpreting genome-wide expression profiles. Proc Natl Acad Sci U S A 2005;102:15545-50.
27. Teo MY, Rosenberg JE. Nivolumab for the treatment of urothelial cancers. Expert Rev Anticancer Ther 2018;18:215-21.
28. WEINHOUSE S. On respiratory impairment in cancer cells. Science 1956;124:267-9.
29. Schiliro C, Firestein BL. Mechanisms of Metabolic Reprogramming in Cancer Cells Supporting Enhanced Growth and Proliferation. Cells 2021;10:1056. Correction in Cells 2022;11:3593.
30. Jain M, Nilsson R, Sharma S, et al. Metabolite profiling identifies a key role for glycine in rapid cancer cell proliferation. Science 2012;336:1040-4.
31. Bartrons R, Caro J. Hypoxia, glucose metabolism and the Warburg's effect. J Bioenerg Biomembr 2007;39:223-9.
32. Cui J, Mao X, Olman V, et al. Hypoxia and miscoupling between reduced energy efficiency and signaling to cell proliferation drive cancer to grow increasingly faster. J Mol Cell Biol 2012;4:174-6.
33. Kastenhuber ER, Lowe SW. Putting p53 in Context. Cell 2017;170:1062-78.
34. Huang R, Li G, Wang Z, et al. Identification of an ATP metabolism-related signature associated with prognosis and immune microenvironment in gliomas. Cancer Sci 2020;111:2325-35.
35. Kesarwani P, Prabhu A, Kant S, et al. Metabolic remodeling contributes towards an immune-suppressive phenotype in glioblastoma. Cancer Immunol Immunother 2019;68:1107-20.
36. Becker JC, Andersen MH, Schrama D, et al. Immune-suppressive properties of the tumor microenvironment.

Cancer Immunol Immunother 2013;62:1137-48.
37. Ghesquière B, Wong BW, Kuchnio A, et al. Metabolism of stromal and immune cells in health and disease. Nature 2014;511:167-76.
38. Oresta B, Pozzi C, Braga D, et al. Mitochondrial metabolic reprogramming controls the induction of immunogenic cell death and efficacy of chemotherapy in bladder cancer. Sci Transl Med 2021;13:eaba6110.
39. Tan AC, Heimberger AB, Khasraw M. Immune Checkpoint Inhibitors in Gliomas. Curr Oncol Rep 2017;19:23.
40. Malta TM, Sokolov A, Gentles AJ, et al. Machine Learning Identifies Stemness Features Associated with Oncogenic Dedifferentiation. Cell 2018;173:338-354.e15.
41. Cruceru ML, Neagu M, Demoulin JB, et al. Therapy targets in glioblastoma and cancer stem cells: lessons from haematopoietic neoplasms. J Cell Mol Med 2013;17:1218-35.
42. Rampazzo E, Del Bianco P, Bertorelle R, et al. The predictive and prognostic potential of plasma telomerase reverse transcriptase (TERT) RNA in rectal cancer patients. Br J Cancer 2018;118:878-86.
43. Zhao L, Zhang J, Liu Z, et al. Identification of biomarkers for the transition from low-grade glioma to secondary glioblastoma by an integrated bioinformatic analysis. Am J Transl Res 2020;12:1222-38.
44. Bien SA, Su YR, Conti DV, et al. Genetic variant predictors of gene expression provide new insight into risk of colorectal cancer. Hum Genet 2019;138:307-26.
45. Rutledge EA, McMahon AP. Mutational analysis of genes with ureteric progenitor cell-specific expression in branching morphogenesis of the mouse kidney. Dev Dyn 2020;249:765-74.
46. Chen C, Wang X, Huang X, et al. Nicotinamide N-methyltransferase: a potential biomarker for worse prognosis in gastric carcinoma. Am J Cancer Res 2016;6:649-63.
47. Roberti A, Fernández AF, Fraga MF. Nicotinamide N-methyltransferase: At the crossroads between cellular metabolism and epigenetic regulation. Mol Metab 2021;45:101165.
48. Khan FU, Owusu-Tieku NYG, Dai X, et al. Wnt/β-Catenin Pathway-Regulated Fibromodulin Expression Is Crucial for Breast Cancer Metastasis and Inhibited by Aspirin. Front Pharmacol 2019;10:1308.
49. Muthana SM, Campbell CT, Gildersleeve JC. Modifications of glycans: biological significance and therapeutic opportunities. ACS Chem Biol 2012;7:31-43.
50. Hao XD, Liu YN, Hu SH, et al. Association of macular corneal dystrophy with excessive cell senescence and apoptosis induced by the novel mutant CHST6. Exp Eye Res 2022;214:108862.
51. Ho WL, Che MI, Chou CH, et al. B3GNT3 expression suppresses cell migration and invasion and predicts favorable outcomes in neuroblastoma. Cancer Sci 2013;104:1600-8.

(English Language Editor: A. Kassem)

Cite this article as: Liu G, Lu Y, Gao D, Huang Z, Ma L. Identification of an energy metabolism-related six-gene signature for distinguishing and forecasting the prognosis of low-grade gliomas. Ann Transl Med 2023;11(3):146. doi: 10.21037/atm-22-6502

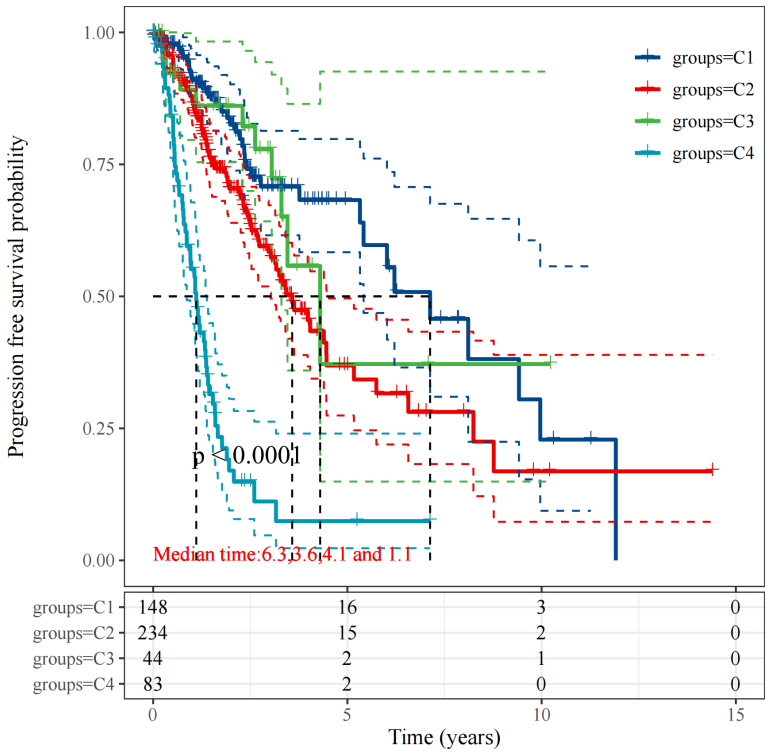

Figure S1 Kaplan-Meier survival curves of progression-free survival in the different clusters.

https://dx.doi.org/10.21037/atm-22-6502